Electron-phonon interaction of one-dimensional and two-dimensional surface states in indium adlayers on the Si(111) surface

Sang Hoon Uhm and Han Woong Yeom*

Department of Physics and Center for Low Dimensional Electronic Symmetry, Pohang University of Science and Technology, Pohang 790-784, Korea

(Received 4 September 2012; published 10 December 2012)

We performed angle-resolved photoelectron spectroscopy measurements on one- and two-dimensional (1D and 2D) metallic surface states in indium layers on the Si(111) surface as a function of temperature. The temperature dependence of surface-state energy widths was used to estimate the electron-phonon coupling constant λ. The 2D metallic surface states of the $\sqrt{7} \times \sqrt{3}$-In layer above one monolayer exhibit $\lambda = 0.8 \sim 1.0$, similar to the value of bulk indium 0.9. This is discussed in the light of a recent structure model with a double indium layer and the relatively high superconducting transition temperature of this surface. On the other hand, the λ's of two 1D surface states of the 4×1-In surface with one monolayer of indium are much higher than that of $\sqrt{7} \times \sqrt{3}$-In, reaching 1.8, which is the largest ever reported for a surface state. The origin of the enhanced electron-phonon coupling and its relationship to the charge-density-wave phase transition of this surface are discussed.

DOI: 10.1103/PhysRevB.86.245408 PACS number(s): 73.20.At, 79.60.Dp, 73.22.Gk

I. INTRODUCTION

The physical properties of low-dimensional systems such as surfaces and ultrathin films can be largely different from those of corresponding bulks due partly to enhanced manybody interactions of their electrons.[1–3] Angle-resolved photoelectron spectroscopy (ARPES) has provided important and direct information on many-body interactions of such low-dimensional systems.[4] In particular, the enhanced electron-phonon coupling (EPC) on metal surfaces and in metal quantum films has been quantified by ARPES.[5–8] These systems have played the role of model systems to investigate the EPC of low-dimensional materials in unprecedented accuracy and details. However, similar studies on semiconductor surfaces and nanostructures are quite few. Nevertheless, the EPC in semiconductor surfaces could be important to elucidate the interaction of electrons with a specific phonon mode[12] and that in semiconductor nanostructures are crucial to understand their optical properties through the behavior of exitons and polarons.[9–11]

In this paper, we focus on the EPC of monolayer (ML)-regime metallic films on a semiconducting substrate, which possess abrupt interfaces and host well isolated one- or two-dimensional (1D and 2D) electronic states due to the substrate band gap. In principle, these electronic systems would exhibit more ideal low-dimensional EPC than surface states of metal surfaces because of the limited coupling to bulk electronic states. In particular, indium layers on the Si(111) surface, the so-called 4×1-In[13] and $\sqrt{7} \times \sqrt{3}$-In[14] surfaces are interesting since they exhibit at low-temperature broken symmetry ground states due to EPC such as charge-density-wave (CDW)[13] and superconducting phases.[15,16]

The 4×1-In layer forms at one ML coverage of In. Indium atoms are incorporated into the Si(111) top layer to form a 1D chain structure; two zigzag In chains separated by silicon zigzag chains constitute a unit cell (see Fig. 1).[17] This surface exhibits three quasi-1D metallic surface states, one half-filled and the others less-than-half filled (see Fig. 2),[13] which could be fully reproduced by band structure calculations based on the above structure model.[18] A metal-insulator phase transition into a periodicity doubled 8×2 phase was reported at 120–130 K and was discussed in terms of Peierls instability and the CDW formation.[13,19] However, the complex band structure with multiple 1D bands has made the interpretation of the phase transition difficult in terms of a simple, single-band, Peierls transition.[20] The atomic structure of the low-temperature phase was determined recently, which in turn revealed the electronic energy gain through the metal-insulator transition may not be significant.[21] Naturally, the order-disorder transition scenario emerged, which interpreted the high temperature phase as a fluctuating state between degenerated 8×2 configurations.[22] This idea was subsequently denied by ARPES,[23,24] core-level photoelectron spectroscopy,[23,25] Raman spectroscopy,[26] and x-ray diffraction measurements.[27] That is, vast experimental evidence has been accumulated to conclude that the metal-insulator transition accompanies a displacive structural distortion and that the structural and electronic degree of freedoms are tightly entangled in this system. Very recently, a theoretical work indicated the importance of the phonon structure and the entropic gain in the free energy in understanding this phase transition.[28] However, even in this most updated theoretical study, the EPC was not fully considered, which calls for further theoretical and experimental studies on the EPC in this system.

On the other hand, at a higher In coverage than one ML, a well-ordered layer with a $\sqrt{7} \times \sqrt{3}$ periodicity forms.[29,30] This surface exhibits a well defined 2D nearly-free-electron band at Fermi level, while its whole band structure with various branch bands was not fully understood.[14] The atomic structure and the exact In coverage of this surface have not been clear with different structure models proposed.[14] The EPC strength was estimated roughly by ARPES to be similar to that of bulk In, which suggested the possibility of the superconducting phase at low, but relatively high, temperature.[14] Very recently, the superconducting transition was indeed observed to occur at 3.18 K, which is surprisingly close to that of the bulk transition temperature 3.4 K against the conventional wisdom of the absence of a long-range superconducting correlation in the 2D

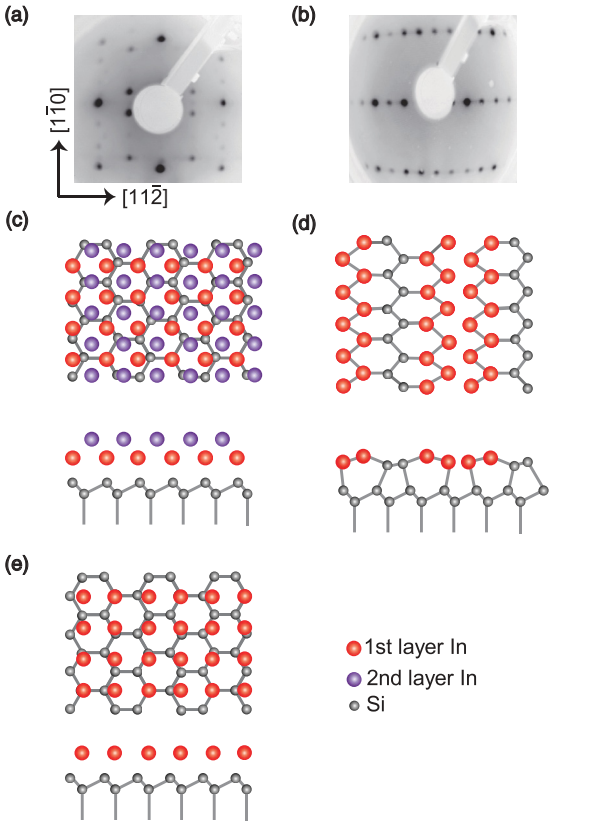

FIG. 1. (Color online) LEED patterns for the (a) $\sqrt{7} \times \sqrt{3}$-In and (b) 4×1-In surfaces. Schematics of the structure models for the $\sqrt{7} \times \sqrt{3}$-In surface with (c) 2.4 ML as proposed recently[37] and (e) 1.2 ML (the so called rectangular $\sqrt{7} \times \sqrt{3}$ model) and the widely accepted model (1.0 ML) for (d) the 4×1-In surface.[17] The side views are along the [11$\bar{2}$] direction.

limit.[15] In contrast to $\sqrt{7} \times \sqrt{3}$-In, a similar 2D layer of Pb on Si(111), $\sqrt{7} \times \sqrt{3}$-Pb, showed the superconducting phase

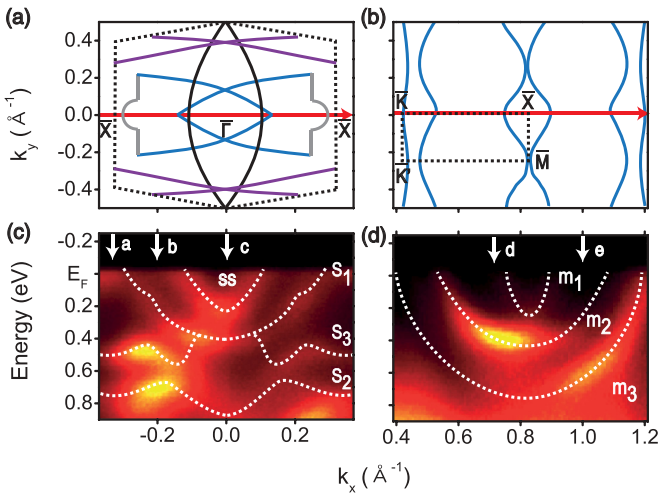

FIG. 2. (Color online) Schematics of Fermi contours for the Si(111)$\sqrt{7} \times \sqrt{3}$-In and (b) 4×1-In surface. The corresponding band dispersions (ARPES intensity maps in color scale) measured along the red lines in (a) and (b) at 130 K are displayed in (c) and (d), respectively. The surface state band dispersions are guided by dashed lines.

only below 1.52 K, reduced significantly from the transition temperature 7.19 K of bulk Pb.[15,31] It is thus obvious that a more detailed study of EPC in these systems is required to understand the origin of the 2D superconducting phase itself and the contrasting behavior between In and Pb layers.

In the present study, we attempted to quantify the EPC of the Si(111)$\sqrt{7} \times \sqrt{3}$-In and Si(111)4×1-In surfaces. We performed detailed ARPES measurements for a few different surface states of two surfaces. The energy widths of the surface states were measured as a function of temperature, which were used to determine the EPC constant λ of specific surface states reliably. Our results clearly indicate that λ is largely different between the $\sqrt{7} \times \sqrt{3}$-In and 4×1-In surfaces. The $\sqrt{7} \times \sqrt{3}$-In surface states show λ similar to bulk In as reported earlier but those of 4×1-In exhibit the substantial enhancement in λ. This enhancement is discussed in terms of the dimensional character of surface state bands and the symmetry-breaking phase transitions found on these surfaces.

II. EXPERIMENTAL METHODS AND STRUCTURE MODELS

An *n*-type Si(111) substrate with a resistivity of 5–10 Ωcm was heated by direct current to obtain a 7×7 reconstruction. A Si(111) substrate with a miscut by 1.9° towards [11$\bar{2}$] was used to avoid the formation of triply rotated domains of 4×1-In and $\sqrt{7} \times \sqrt{3}$-In due to their reduced rotational symmetry.[14,32] After depositing In of larger than 2 ML on Si(111)7×7, various surface reconstructions were formed by post annealings at different temperatures to remove the excess In.[33] Annealing to 500 K, we observed the low-energy-electron diffraction (LEED) pattern of a single domain $\sqrt{7} \times \sqrt{3}$-In surface as shown in Fig. 1(a). Further annealing of the $\sqrt{7} \times \sqrt{3}$-In surface at about 600 K leaded to the formation of a single domain 4×1-In surface [see Fig. 1(b)].

Atomic structure models of these surfaces are shown in Fig. 1. As mentioned above, the 4×1-In surface is composed of alternating zigzag chains of In and Si atoms [Fig. 1(d)]. This structure model is well supported by the total energy calculations,[18,34] the LEED *I-V* analysis,[35] and the x-ray diffraction data[17] as well as the comparison of various experimental data such as band dispersions,[13] scanning tunneling microscopy images,[19] and optical absorption spectra[36] with those calculated based on the model. This structure undergoes a displacive phase transition into a 8×2 structure below 125 K, where the two In zigzag chains are rearranged into hexagons.[13,21,28] On the other hand, the atomic structure of the $\sqrt{7} \times \sqrt{3}$-In surface is rather uncertain. Two structure models with 1.2 ML of In were proposed, which are called the hexagonal and rectangular $\sqrt{7} \times \sqrt{3}$ structures [Fig. 1(e)].[29,30] These models are simply based on the interpretation of the apparent STM images but little conclusive evidence has been available to pin down one model. In sharp contrast, a recent total-energy calculation suggested that a new structure, the double In layer structure (each layer with 1.2 ML of In) [Fig. 1(c)], is energetically favored over the previous single layer models.[37] Moreover, it was clarified that only the double In layer model can properly reproduce the experimental band dispersions.[37]

For ARPES measurements, a high-performance electron analyzer (R4000, VG Scienta, Sweden) was utilized with a He

I_α discharge radiation ($h\nu = 21.2$ eV). The band dispersions were measured from 100 to 300 K. The angle and energy resolutions were 0.15° and 15 meV at best. LEED patterns were used to check the surface order and to ensure consistent surfaces for repeated surface preparations.

III. RESULTS AND DISCUSSION

A. The Si(111)$\sqrt{7} \times \sqrt{3}$-In surface

Figure 2(a) shows the schematic Fermi contour reported previously and the ARPES intensity map measured along the $[1\bar{1}0]$ direction of the $\sqrt{7} \times \sqrt{3}$-In surfaces at 130 K. For the $\sqrt{7} \times \sqrt{3}$-In surface, the ARPES map is taken crossing one $\overline{\Gamma}$ point of the surface Brillouin zone (SBZ). This particular k span shows most of the surface states with better clarity in ARPES. The Fermi contours of $\sqrt{7} \times \sqrt{3}$-In are mainly composed of the traces of a 2D free electron circle (one parabolic band) [solid lines in Fig. 2(a)] overlapped according to the $\sqrt{7} \times \sqrt{3}$ periodicity.[14] In the band map, this Fermi contour corresponds to the surface state denoted ss. Other surface states, S_1 (corresponding to the Fermi contours in gray lines), S_2, and S_3, were assumed to come from In-Si bonds at the interface. The Fermi contours and the underlying band structure of $\sqrt{7} \times \sqrt{3}$-In are well reproduced in a recent calculation based on the double layer model.[37] The above interpretation for the surface state bands is roughly consistent with this calculation, while the calculation discloses more complicated origin of each band. The S_1 state largely comes from the in-plane In-In bonding in the second In layer while the S2 and S3 bands mostly from the interfacial In-Si bonds. The ss state would be a result of the overlap of two adjacent bands due to the electronic state localized on the first (top) In layer and that representing the bonds between the two In layers. Even for the ss state, there is a strong hybridization with the interfacial In-Si state when its energy deviates from the Fermi level, that is, near the $\overline{\Gamma}$ point. Thus, in the present study, we treat most of the surface states observed except for S1 and ss near the Fermi energy as due to the In-Si bonds. At the particular photon energy used, we could not clearly resolve out another surface state due to the first In layer, which was rather prominent in the previous ARPES study[14] performed with a much higher photon energy of 100 eV. We attribute this to the variation of the photoemission crossection or matrix elements due to a large difference in the exciting photon energy. Indeed, substantial differences are noticed for spectral weights of most of the surface states while their dispersions are consistent in the previous and present works.[14]

In order to determine EPC constants λ's of the $\sqrt{7} \times \sqrt{3}$-In surface, we carried out temperature-dependent ARPES measurements. It is well established that at sufficiently high temperatures as in the present experiment, the temperature-dependent part of the lifetime of a surface-state photohole τ_{hole} is mainly governed by the photohole decay through the coupling with phonons. Then, the temperature dependence of τ_{hole} is given by $\hbar/\tau_{\text{hole}} = 2\pi\lambda k_B T$ (k_B is the Boltzmann constant) and the spectral width of a surface-state band ΔE, inversely proportional to τ_{hole}, depends linearly on the temperature.[8,38] Thus the EPC constant λ can be extracted

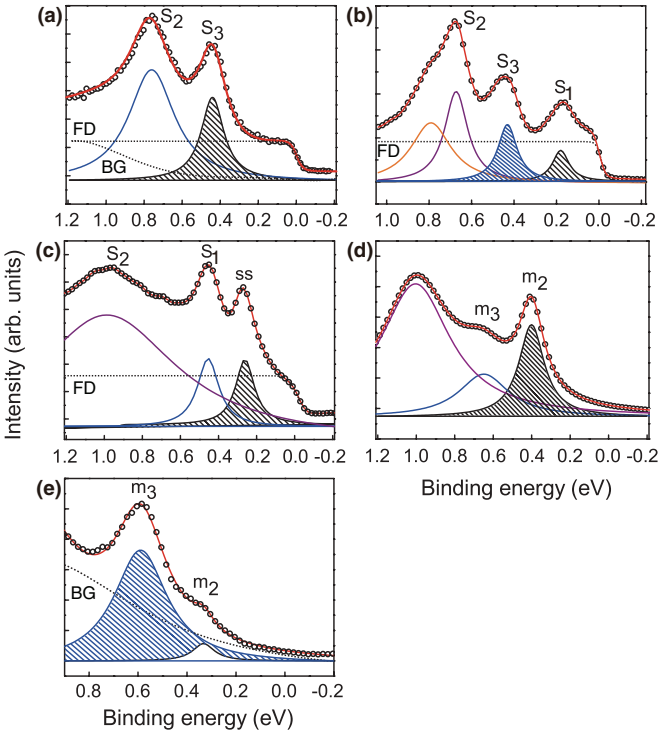

FIG. 3. (Color online) Selected ARPES energy distribution curves for different surface states at different k_x indicated by arrows in Figs. 2(c) and 2(d) taken at 130 K. These curves are fitted with multiple Lorentzian functions (shown in the figure) and the Fermi-Dirac (FD) function and smooth polynomial backgrounds (BG) to extract the spectral width of each surface state. The results of the fits are overlapped as solid lines on the raw data in open circles. The widths of relatively sharp and well separated surface-state features, those with hatchings, were analyzed further for their temperature dependence.

from the slope of the temperature dependence of ΔE:[8,38]

$$\lambda = \frac{1}{2\pi k_B}\frac{d\Delta E}{dT}. \quad (1)$$

For the measurements of ΔE, we chose energy distribution curves (EDC's) at several different k points [indicated by the arrows in Fig. 2(a)]. The spectral width in EDC becomes very broad and is not reliably fit for a k point where the surface-state band exhibits a steep dispersion. Thus we selected k points where the surface states show only gentle dispersions. The selected EDC's are shown in Figs. 3(a)–3(c), which were then fit by Lorentzian functions with smooth (polynomial) backgrounds and a Fermi-Dirac function.[12] The resulting Lorentzian linewidths for a few surface states are displayed in Fig. 4(a) as a function of temperature. Indeed, the spectral widths of surface states extracted experimentally increase monotonically with the increase of temperature, which are fit well by a linear function within the experimental uncertainty. The obtained EPC constant λ values are 0.80 ± 0.17 (ss), 1.02 ± 0.16 (S_1), 0.96 ± 0.13 ($S_3{}^a$), 0.88 ± 0.17 ($S_3{}^b$). The width of the S2 state with a high binding energy of about 0.8 eV was too broad for a similar analysis. The corresponding photohole lifetime τ_{hole} at 300 K varies between 3.9×10^{-15} and 5.0×10^{-15} s as summarized in Table I.

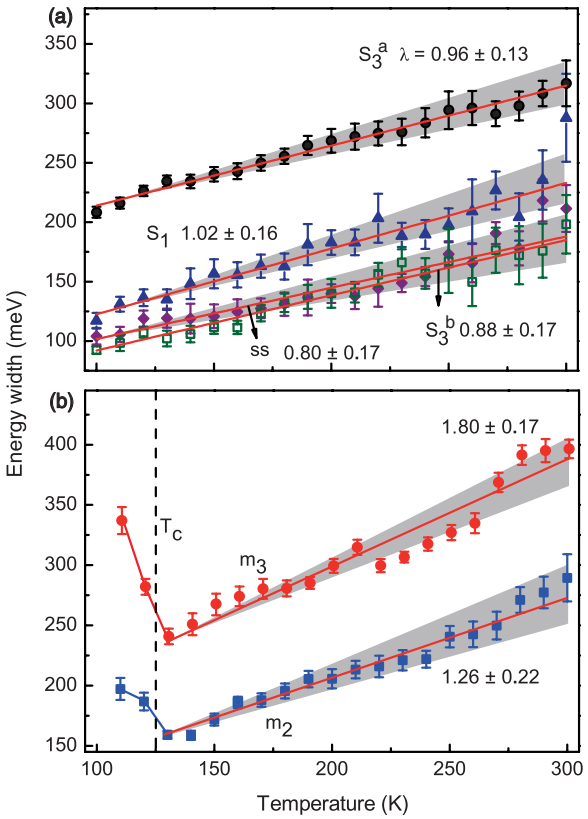

FIG. 4. (Color online) The Lorentzian energy widths of the surface states of the (a) $\sqrt{7} \times \sqrt{3}$-In and (b) 4×1-In surfaces are plotted as a function of temperature. From the linear fit of each set of data the corresponding electron-phonon coupling constant λ was obtained as indicated. For the S3 state, the width data were taken at two different k points (in-plane electron momenta), indicated by a and b arrows in Fig. 2(c), which are marked as $S3^a$ and $S3^a$, respectively. The possible range of the linear fits are indicated by shadows, which was used to conservatively estimate the uncertainty in quantifying λ.

The EPC constants λ's of ss, S_1, and S_3 bands vary between 0.8 and 1.0 around the corresponding bulk value of 0.9 ± 0.1. In principle, the EPC constant can vary from band to band and from one k point to the other for a single band due to different density of states (DOS) of electrons and phonons.[39] The k dependence of a single band was examined for S_3, which exhibits λ of 0.88 and 0.96 at two different k points. This variation is smaller than the difference between different bands. In general, the λ value (the photohole relaxation time τ_{hole}) is mostly smaller than unity (larger than $10^{-14} \sim 10^{-15}$ s) for bulk metals, while it often becomes larger at surfaces.[38] This enhancement can come from the enhanced electron DOS near Fermi energy,[40] which is due to the change of Fermi surface (band) geometry from 3D to 2D. In addition, in 2D systems, the lack of 3D screening of electrons can also help to enhance the EPC. However, such a surface enhancement is not noticeable in the surface states of $\sqrt{7} \times \sqrt{3}$-In. The recent observation of the relatively high-superconducting T_c (94% of the bulk value) of the $\sqrt{7} \times \sqrt{3}$-In surface, thus cannot be explained by the enhanced EPC. Note that the single layer of Pb on the same substrate exhibited a much reduced T_c, 1.52 K, only 21% of the bulk value.[15] We suggest that the relatively high T_c of $\sqrt{7} \times \sqrt{3}$-In is due to the fact that this structure is composed of the double In layer as indicated by a recent calculation.[37] In the case of Pb, the double layer has a T_c of 3.65 ± 0.15 K, reaching to 51% of bulk value.[41] While the increasing trend of T_c with respect to the increase in the film thickness is consistent for Pb, the high T_c of the In double layer, $\sqrt{7} \times \sqrt{3}$-In, is outstanding. The recent calculation further showed that even at this thickness the DOS of $\sqrt{7} \times \sqrt{3}$-In are surprisingly close to that of bulk In. This must be related to the very high T_c. A more detailed discussion on the EPC and its influence on the 2D superconductivity requires the information on the phonon DOS, which is not available at present.

B. The Si(111)4 × 1-In surface

Figure 2(b) shows the schematic Fermi contours reported previously and the ARPES intensity map measured along the $[1\bar{1}0]$ direction of the 4×1-In surfaces at 130 K. For the 4×1-In surface, the ARPES map is taken crossing one $\overline{X}$ point

TABLE I. Electron-phonon coupling constant λ, photohole lifetime τ_{hole} (at 300 K) of the surface states measured in the present experiments, and the compilation of the experimental values of the electron-phonon coupling constant λ for other surface systems.

Surface	Phase	State	Photohole lifetime τ_{hole}	λ (surface)	λ (bulk)	Reference
Our experiments						
In/Si(111)	$\sqrt{7} \times \sqrt{3}$	ss	5.0×10^{-15} s	0.80 (±0.17)	0.9 (±0.1)	42
		S_1	3.9×10^{-15} s	1.02 (±0.16)	0.9 (±0.1)	42
		S_3^a	4.2×10^{-15} s	0.96 (±0.13)	0.9 (±0.1)	42
		S_3^b	4.5×10^{-15} s	0.88 (±0.17)	0.9 (±0.1)	42
In/Si(111)	4×1	m_2	3.2×10^{-15} s	1.26 (±0.22)	0.9 (±0.1)	42
		m_3	2.2×10^{-15} s	1.80 (±0.17)	0.9 (±0.1)	42
Other experiments						
Pb/Si(111)	$\sqrt{3} \times \sqrt{3}$			1.07 (±0.13)	1.41	15,43
Be(0001)				1.15	0.24	38
Be(1010)				0.65 ± 0.02	0.24	44
Bi(001)				0.3 ∼ 1.0	−0.13	45
Cu(110)				0.23 ± 0.02	0.15	46
V(001)				1.45	−0.4	47
Ag/Fe(100)				0.3 ∼ 1.0	0.15	48

of the corresponding SBZ. The origins of the metallic surface states of the 4 × 1-In surface are simpler and well understood. As shown in Figs. 2(b) and 2(d), there exist three partially filled metallic bands. The m_3 band is a half-filled band and is close to an ideal 1D band with a minimal dispersion perpendicular to In chains. The other bands m_1 and m_2 have substantial dispersions perpendicular to the wires and are almost degenerated around the $\overline{\mathrm{M}}$ point. The calculations confirmed that these metallic states are due largely to in-plane In-In bonds within the In chains.[18,34]

We also performed temperature-dependent ARPES measurements for determination of EPC constant λ's of the 4 × 1-In surface. When we fit EDCs of the 4 × 1-In surface at selected k points in Fig. 2(d), only the temperature-independent smooth (polynomial) backgrounds were needed. The obtained EPC constant λ values are 1.26 ± 0.22 (m_2) and 1.80 ± 0.17 (m_3). The corresponding photohole lifetime τ_{hole} at 300 K varies between 2.2×10^{-15} and 3.2×10^{-15} s as summarized in Table I.

What is contrasting is that the EPC constant λ of the m_3 surface state of the 4 × 1-In surface is as large as 1.8. This is the largest value ever observed in surface systems.[8] The surface to bulk ratio of λ or the surface enhancement itself is not too surprising since the enhancement up to 300–400% was observed previously on metal surfaces such as V and Be.[38,47] Note also that all the previous measurements were done on surface states with 2D dispersions while the m_3 band has an almost ideal 1D dispersion. On the other hand, the λ value of m_2 state on the same surface is much smaller as 1.3, but still significantly larger than the bulk value. From this, we speculate that the diversified λ value is due mainly to the dimensional character of the surface state bands. As shown in Fig. 2, the m_3 band has an almost ideal 1D dispersion while m_2 has a substantial 2D modulation. In order to provide a little bit more quantitative measure, we calculated the DOS at the measured k points using the experimentally determined band dispersions. We first fit the measured band dispersions by a function $E(k) = E_0 + \frac{\hbar^2}{2m_x^*}k_x^2 + \frac{\hbar^2}{2m_y^*}k_y^2$, which then provides the DOS values by a formula of $\int 1/[2\pi^2|\nabla E(k_x,k_y)|]dk$ (the integration over a 2D k-space line with the span of the experimental resolution of 0.01 $\mathrm{\AA}^{-1}$). The calculated DOS of a nearly ideal 1D band of the m_3 band at the selected k point is 1.7×10^{-2}/eV, which is about 1.2 times that of the quasi 1D band m_2 at the selected k point and 2.7 times that of an isotropic 2D parabolic band. Therefore it seems reasonable to attribute the main difference between the m_2's and m_3's EPC to their band dispersions and DOS while we assume the phonon parts are not substantially different for these two closely lying bands. In principle, a large difference in the EPC of different bands of the same material is in fact not unusual due to the largely varying DOS and phonon spectrum from band to band and for different energy and momentum values. Indeed, a recent state-of-the-art calculation showed that the EPC strength can vary by up to four times for different bands of bulk Pb.[39]

While the present measurements utilized ARPES, the recent surface transport measurements also reported the EPC values. The λ values reported are 0.77 and 2.36, along and perpendicular to the chains, respectively, for 4×1-In (as calculated from the τ_{hole} value reported)[49] and 1.2 for $\sqrt{7} \times \sqrt{3}$-In.[50] If we assume that the ARPES values averaged over different bands correspond to the transport values averaged over different directions, then the present and the transport measurements are roughly consistent for the 4 × 1-In case. The discrepancy for the $\sqrt{7} \times \sqrt{3}$-In surface is not substantial considering the experimental errors. We note that the transport measurement confirms the enhanced EPC for the 1D surface state of 4×1-In in agreement with the present work.

The large EPC strength of the half-filled 1D band of m_3 may indicate that the EPC is important for the metal-insulator transition above 120 K accompanying a displacive structural distortion. While the recent theoretical study indicated the important contribution of the phonon degree of freedom in this phase transition,[28] the EPC contribution was not fully investigated yet. Since such a quantitative study of the EPC is possible with the first-principles calculations of the phonon spectrum and the evaluation of the Eliashberg function,[51] a further theoretical study would provide a clearer insight into the mechanism of this phase transition.

It is noteworthy that the apparent widths of surface states increase below the transition temperature of 120–130 K for the metal-insulator transition in clear contrast to the monotonic decrease from room temperature to this temperature. Below 110 K or so, the band structure is replaced by two fully gapped bands of the 8 × 2 structure.[20,24] Thus one cannot trace the width of the metallic surface states at a lower temperature. The increase of the width just below 125 K is understood from the extra fluctuation during the phase transition such as the mixture of metallic and insulating domains[19] and the critical fluctuations. This behavior, the apparent reduction of the width near the transition temperature, is not easily compatible with the order-disorder transition scenario for the phase transition, where the fluctuation increases gradually and continuously (thus cannot be suppressed at a certain temperature range) as the temperature increases. This conclusion is consistent with the other recent experimental evidences such as x-ray diffraction and optical spectroscopy measurements[27,36] as well as the abrupt change of the band structure itself at the transition temperature.[23,24]

IV. CONCLUSIONS

We performed temperature-dependent ARPES measurements for the metallic In adlayers grown on the Si(111) surface. We quantified the electron-phonon coupling constants λ's of the quasi 1D surface states of the 4 × 1-In surface at one ML and the 2D surface states of the $\sqrt{7} \times \sqrt{3}$-In surface formed at a higher In thickness. The λ values of the 2D surface states of the $\sqrt{7} \times \sqrt{3}$-In surface vary between 0.8 and 1.0 being very close to that of bulk In 0.9.[14] This is thought to be related to the very much bulklike DOS characteristics of the double layer $\sqrt{7} \times \sqrt{3}$-In structure disclosed in a recent theoretical study.[37] This can also explain the relatively high superconducting transition temperature of this surface, which is fairly close to the bulk transition temperature. In sharp contrast, the electron-phonon coupling strength of the quasi-1D metallic surface states of the 4 × 1-In surface was found to be substantially enhanced from the bulk value as 1.3 and even 1.8 for an ideally 1D half-filled band. This enhancement can largely be explained by the enhanced DOS

due to the change of the band (Fermi surface) geometry from 2D (or 3D) to quasi-1D and 1D. The role of the enhanced electron-phonon coupling of the half-filled metallic band in the periodicity-doubling metal-insulator transition is required to be investigated further, in particular, by theoretical calculations of the phonon spectrum and the Eliashberg function.

ACKNOWLEDGMENTS

This work was supported by MOST through Center for Low-dimensional Electronic Symmetry of the CRi program. The authors appreciate the discussion with M. H. Kang.

*yeom@postech.ac.kr

[1] C. Zeng, P. R. C. Kent, T.-H. Kim, A.-P. Li, and H. H. Weitering, Nat. Mater. **7**, 539 (2008).
[2] V. Vescoli, L. Degiorgi, W. Henderson, G. Grüner, K. P. Starkey, and L. K. Montgomery, Science **281**, 1181 (1998).
[3] H. Shishido, T. Shibauchi, K. Yasu, T. Kato, H. Kontani, T. Terashima, and Y. Matsuda, Science **327**, 980 (2010).
[4] A. Damascelli, Z. Hussain, and Z.-X. Shen, Rev. Mod. Phys. **75**, 473 (2003).
[5] B. A. McDougall, T. Balasubramanian, and E. Jensen, Phys. Rev. B **51**, 13891 (1995).
[6] A. Eiguren, B. Hellsing, F. Reinert, G. Nicolay, E. V. Chulkov, V. M. Silkin, S. Hüfner, and P. M. Echenique, Phys. Rev. Lett. **88**, 066805 (2002).
[7] J. J. Paggel, T. Miller, and T.-C. Chiang, Phys. Rev. Lett. **83**, 1415 (1999).
[8] E. W. Plummer, J. Shi, S.-J. Tang, E. Rotenberg, and S. D. Kevan, Prog. Surf. Sci. **74**, 251 (2003).
[9] G. Khitrova, H. M. Gibbs, M. Kira, S. W. Koch, and A. Scherer, Nat. Phys. **2**, 81 (2006).
[10] S. W. Koch, M. Kira, G. Khitrova, and H. M. Gibbs, Nat. Mater. **5**, 523 (2006).
[11] S. W. Koch, T. Meier, W. Hoyer, and M. Kira, Physica E **14**, 45 (2002).
[12] I. Barke, Fan Zheng, A. R. Konicek, R. C. Hatch, and F. J. Himpsel, Phys. Rev. Lett. **96**, 216801 (2006).
[13] H. W. Yeom, S. Takeda, E. Rotenberg, I. Matsuda, K. Horikoshi, J. Schaefer, C. M. Lee, S. D. Kevan, T. Ohta, T. Nagao, and S. Hasegawa, Phys. Rev. Lett. **82**, 4898 (1999).
[14] E. Rotenberg, H. Koh, K. Rossnagel, H. W. Yeom, J. Schäfer, B. Krenzer, M. P. Rocha, and S. D. Kevan, Phys. Rev. Lett. **91**, 246404 (2003).
[15] T. Zhang, P. Cheng, W.-J. Li, Y.-J. Sun, G. Wang, X.-G. Zhu, K. He, L. Wang, X. Ma, X. Chen, Y. Wang, Y. Liu, H.-Q. Lin, J.-F. Jia, and Q.-K. Xue, Nat. Phys. **6**, 104 (2010).
[16] T. Uchihashi, P. Mishra, M. Aono, and T. Nakayama, Phys. Rev. Lett. **107**, 207001 (2011).
[17] O. Bunk, G. Falkenberg, J. H. Zeysing, L. Lottermoser, R. L. Johnson, M. Nielsen, F. Berg-Rasmussen, J. Baker, and R. Feidenhansl, Phys. Rev. B **59**, 12228 (1999).
[18] J.-H. Cho, D.-H. Oh, K. S. Kim, and L. Kleinman, Phys. Rev. B **64**, 235302 (2001).
[19] S. J. Park, H. W. Yeom, S. H. Min, D. H. Park, and I.-W. Lyo, Phys. Rev. Lett. **93**, 106402 (2004).
[20] J. R. Ahn, J. H. Byun, H. Koh, E. Rotenberg, S. D. Kevan, and H. W. Yeom, Phys. Rev. Lett. **93**, 106401 (2004).
[21] C. González, F. Flores, and J. Ortega, Phys. Rev. Lett. **96**, 136101 (2006).
[22] C. González, J. Guo, J. Ortega, F. Flores, and H. H. Weitering, Phys. Rev. Lett. **102**, 115501 (2009).
[23] J. R. Ahn, J. H. Byun, J. K. Kim, and H. W. Yeom, Phys. Rev. B **75**, 033313 (2007).
[24] Y. J. Sun, S. Agario, S. Souma, K. Sugawara, Y. Tago, T. Sato, and T. Takahashi, Phys. Rev. B **77**, 125115 (2008).
[25] H. W. Yeom, K. Horikoshi, H. M. Zhang, K. Ono, and R. I. G. Uhrberg, Phys. Rev. B **65**, 241307 (2002).
[26] K. Fleischer, S. Chandola, N. Esser, W. Richter, and J. F. McGilp, Phys. Rev. B **76**, 205406 (2007).
[27] S. Hatta, Y. Ohtsubo, T. Aruga, S. Miyamoto, H. Okuyama, H. Tajiri, and O. Sakata, Phys. Rev. B **84**, 245321 (2011).
[28] S. Wippermann and W. G. Schmidt, Phys. Rev. Lett. **105**, 126102 (2010).
[29] J. Kraft, S. L. Surnev, and F. P. Netzer, Surf. Sci. **340**, 36 (1995).
[30] J. Kraft, M. G. Ramsey, and F. P. Netzer, Surf. Sci. **372**, L271 (1997).
[31] B. T. Matthias, T. H. Geballe, and V. B. Compton, Rev. Mod. Phys. **35**, 1 (1963).
[32] J. L. Stevens, M. S. Worthington, and I. S. T. Tsong, Phys. Rev. B **47**, 1453 (1993).
[33] V. G. Lifshits, A. A. Saranin, and A. V. Zotov, *Surface Phases on Silicon* (Wiley, West Sussex, 1994).
[34] J. Nakamura, S. Watanabe, and M. Aono, Phys. Rev. B **63**, 193307 (2001).
[35] S. Mizuno, Y. O. Mizuno, and H. Tochihara, Phys. Rev. B **67**, 195410 (2003).
[36] E. Speiser, S. Chandola, K. Hinrichs, M. Gensch, C. Cobet, S. Wippermann, W. G. Schmidt, F. Bechstedt, W. Richter, K. Fleischer, J. F. McGilp, and N. Esser, Phys. Status Solidi B **247**, 2033 (2010).
[37] J. H. Park and M. H. Kang, Phys. Rev. Lett. **109**, 166102 (2012).
[38] T. Balasubramanian, E. Jensen, X. L. Wu, and S. L. Hulbert, Phys. Rev. B **57**, R6866 (1998).
[39] I. Yu. Sklyadneva, R. Heid, P. M. Echenique, K.-B. Bohnen, and E. V. Chulkov, Phys. Rev. B **85**, 155115 (2012).
[40] W. L. McMillan, Phys. Rev. **167**, 331 (1968).
[41] S. Qin, J. Kim, Q. Niu, and C.-K. Shih, Science **324**, 1314 (2009).
[42] S. P. Rudin, R. Bauer, A. Y. Liu, and J. K. Freericks, Phys. Rev. B **58**, 14511 (1998).
[43] J. Noffsinger and M. L. Cohen, Phys. Rev. B **81**, 214519 (2010).
[44] S.-J. Tang, Ismail, P. T. Sprunger, and E. W. Plummer, Phys. Rev. B **65**, 235428 (2002).
[45] J. E. Gayone, S. V. Hoffmann, Z. Li, and Ph. Hofmann, Phys. Rev. Lett. **91**, 127601 (2003).
[46] P. Straube, F. Pforte, T. Michalke, K. Berge, A. Gerlach, and A. Goldmann, Phys. Rev. B **61**, 14072 (2000).
[47] M. Kralj, A. Šiber, P. Pervan, M. Milun, T. Valla, P. D. Johnson, and D. P. Woodruff, Phys. Rev. B **64**, 085411 (2001).

[48] D.-A. Luh, T. Miller, J. J. Paggel, and T.-C. Chiang, Phys. Rev. Lett. **88**, 256802 (2002).
[49] T. Kanagawa, R. Hobara, I. Matsuda, T. Tanikawa, A. Natori, and S. Hasegawa, Phys. Rev. Lett. **91**, 036805 (2003).
[50] S. Yamazaki, Y. Hosomura, I. Matsuda, R. Hobara, T. Eguchi, Y. Hasegawa, and S. Hasegawa, Phys. Rev. Lett. **106**, 116802 (2011).
[51] H. J. Choi, D. Roundy, H. Sun, M. L. Cohen, and S. G. Louie, Phys. Rev. B **66**, 020513 (2002).